

**CHANGES IN CORTICAL RESPONSES CAUSED BY LEARNING NOVEL  
OPTOGENETIC STIMULI**

by

Paul Kristian LaFosse

A Thesis

Submitted to the  
Graduate Faculty  
of

George Mason University  
in Partial Fulfillment of

The Requirements for the Degree  
of  
Master of Science  
Biology

Committee:

---

Dr. Ancha Baranova, Committee Chair

---

Dr. Mark Histed, Committee Co-Chair and  
Member

---

Dr. Theodore Dumas, Committee Member

---

Dr. Iosif Vaisman, Acting Director, School  
of Systems Biology

---

Dr. Donna M. Fox, Associate Dean, Office  
of Student Affairs & Special Programs,  
College of Science

---

Dr. Peggy Agouris, Dean, College of  
Science

Date: \_\_\_\_\_

Spring Semester 2019  
George Mason University  
Manassas, VA

Changes in Cortical Responses Caused by Learning Novel Optogenetic Stimuli

A Thesis submitted in partial fulfillment of the requirements for the degree of Master of Science at George Mason University

by

Paul Kristian LaFosse  
Bachelor of Arts  
University of North Carolina at Chapel Hill, 2015

Director: Ancha Baranova, Associate Professor  
School of Systems Biology

Spring Semester 2019  
George Mason University  
Fairfax, VA

Copyright 2018 Paul Kristian LaFosse

All Rights Reserved

## **DEDICATION**

I dedicate this work to my family - my mother, my father, and my brother - for their endless and unwavering support during my time spent away from home. I also dedicate this thesis to my late grandfather, Hallet LaFosse, who taught me early on to strive to see the world from a different perspective.

## **ACKNOWLEDGMENTS**

First, I would like to extend my gratitude to Dr. Mark Histed for his support, guidance, and mentorship throughout my thesis work and for allowing me the opportunity to work in his lab. I also give thanks to the members of the lab, past and present, who have supported me in my training and work. Particularly, I would like to thank Samuel Duffy and Lauren Ryan for their extensive contributions to the project from the start.

I would like to thank Dr. Ancha Baranova for her support and eagerness to work with me in my educational pursuits throughout the program. Additionally, I would like to thank Dr. Theodore Dumas for his guidance and input in my thesis work and Dr. Nathalia Peixoto for other scientific training during my thesis.

Last, I give thanks to the institutions supporting my research and educational training: the School of Systems Biology at George Mason University and the National Institute of Mental Health.

## TABLE OF CONTENTS

	Page
List of Tables .....	vii
List of Figures .....	viii
List of Abbreviations and Symbols.....	ix
Abstract.....	x
Introduction.....	1
Perceptual Learning .....	1
Cortical and Subcortical Targets from Primary Visual Cortex.....	3
Two-Photon Calcium Imaging and Optogenetic Tools .....	4
Hypothesis.....	7
Study Design.....	8
Study Aims .....	10
Methodology .....	11
Materials .....	11
Mouse Rearing and Surgical Preparation .....	11
Visual Detection Task.....	12
Two-Photon Imaging .....	14
Retinotopy.....	15
Visual Response Imaging .....	16
One-Photon Stimulation Detection Task .....	16
Behavior Data Analysis .....	17
Image Analysis and Spike Inference .....	18
Visual Response Analysis - Direction Stimuli .....	19
Results.....	22
Reaction Times Decrease as Animals Learn to Detect an Optogenetic Stimulus .....	22
Animals Improve Sensitivity to Optogenetic Stimulation as Training Progresses.....	25

Neuron Responses in V1 Adapt to Support Learning of an Optogenetic Stimulus.....	27
Discussion.....	31
Conclusion .....	35
References.....	37
Biography.....	41

## **LIST OF TABLES**

Table	Page
Table 1 Laser intensities used across control stimulation experiments .....	9
Table 2 Reaction time analysis parameters for individual animals .....	23

## LIST OF FIGURES

Figure	Page
Figure 1 Timeline of behavior, imaging, and control experiments.....	9
Figure 2 Animal preparation and behavior task structure.....	14
Figure 3 Animals reduce their reaction time to optogenetic stimuli early in learning .....	24
Figure 4 Sensitivity to stimulus intensity improves across learning.....	26
Figure 5 Two-photon calcium imaging of neuron responses to visual stimuli allow quantification of tuning properties.....	29
Figure 6 Learning an optogenetic stimulus induces changes in V1 neuron selectivity and responsivity at the site of stimulation .....	30
Figure 7 Repeated stimulation of opsin does not induce changes in selectivity or responsivity in V1 neurons .....	30

## LIST OF ABBREVIATIONS AND SYMBOLS

Anterolateral .....	AL
Centimeter.....	cm
Change in fluorescence.....	dF
Constrained nonnegative matrix factorization.....	CNMF
Direction selectivity index .....	DSI
Field of view .....	FOV
Flip-excision .....	FLEX
Fluorescence .....	F
Functional magnetic resonance imaging.....	fMRI
Genetically-encoded calcium indicator.....	GECI
Global orientation selectivity index .....	gOSI
Greater than.....	>
Internal ribosome entry site .....	IRES
Intraparietal sulcus .....	IPS
Lateral geniculate nucleus.....	LGN
Lateral-intraparietal.....	LIP
Less than .....	<
Medial-temporal.....	MT
Mediolateral .....	ML
Millisecond .....	ms
MilliWatt.....	mW
Moveable objective microscope .....	MOM
P-value .....	p
Plus or minus .....	±
Posteromedial.....	PM
Primary visual cortex .....	V1
Second.....	s
Secondary visual cortex .....	V2
Standard error of the mean.....	SEM
Superior colliculus .....	SC
Visual area 3 .....	V3
Visual area 4 .....	V4
Visual perceptual learning .....	VPL

## **ABSTRACT**

### **CHANGES IN CORTICAL RESPONSES CAUSED BY LEARNING NOVEL OPTOGENETIC STIMULI**

Paul Kristian LaFosse, M.S.

George Mason University, 2019

Thesis Director: Dr. Mark Histed

Repeated experience with a sensory stimulus can cause perceptual learning, with cerebral cortical responses changing as behavioral improvement occurs. However, since sensory stimuli change the activity of neurons in many different areas of the brain, it has been unclear whether learning creates changes in the cortex, or whether changes in cortical activity reflect changes in afferent input. Here, to determine whether learning-related changes happen directly in local cortical circuits or if all changes occur in downstream areas, we take advantage of the fact animals can learn to base their behavior on non-natural (“off-manifold”) activity patterns evoked by direct stimulation, which allows us to reliably induce stimulation in the same cortical neurons on repeated trials, bypassing afferent areas. We trained mice to detect and report the presence of neural activity evoked by optogenetic stimulation (ChrimsonR in excitatory neurons of primary visual cortex, V1), and found large behavioral improvements as animals learned to detect this stimulus. Animals were first trained to detect a visual stimulus of varying contrast. An optogenetic stimulus was

then paired with every visual stimulus. When performance increased for the lowest contrast visual stimulus, the visual stimulus was turned off and animals performed the task based on the optogenetic stimulus alone. As animals gained experience with the optogenetic stimulus presented alone, animals' reaction time decreased ( $-15.9 \pm 3.8$  ms, per training session, median $\pm$ SEM,  $p < 0.01$ ,  $N = 9$  mice), and detection performance to the stimulus intensity improved (by over an order of magnitude). We imaged calcium responses in local V1 neurons before and after learning (before the optogenetic stimulus is presented and after animals' detection performance for the optogenetic stimulus improved) and found changes in local cortical activity. Visual selectivity for direction and orientation was decreased by optogenetic learning, but overall neural responses became larger. These data suggest local cortical circuitry does adapt to support learning and that cortical processing of one type of stimulus (an ‘on-manifold’ visual stimulus) is degraded by learning another type of stimulus (an “off-manifold” optogenetic stimulus), while neural responses can be enhanced.

## INTRODUCTION

### Perceptual Learning

Perceptual learning is the long-lasting improvement in our ability to perceive, i.e. through a sensory modality such as sight or hearing, with repeated experience to sensory stimuli (Gold and Watanabe, 2013). Because perceptual learning infers that sensory systems in the brain can readily adapt to promote improved behavior, even in adulthood, it provides a useful modality to begin to uncover the neural mechanisms behind how animals process sensory signals for survival. Indeed, many studies over the years have developed and utilized perceptual learning tasks to investigate behavior and neuronal function within specific sensory systems - ranging from early studies in humans with touch sensation to more recent and advanced techniques involving micro-stimulation or patterned two-photon holographic illumination to drive activity in specific subsets of neurons (Gold and Watanabe, 2013; Goldstone, 1998; Ni and Maunsell, 2010; Lerman et al., 2018).

In particular, the visual system has provided a key point of focus for investigating neural activity across learning in perceptual behavior tasks, in part due to an early understanding of the visual system's organization (Fellman and Van Essen, 1991) and the early development of a visual texture discrimination behavior task for assessing perceptual learning effects (Karni and Sagi, 1991). Visual perceptual learning (VPL) is characterized as the marked enhancement in behavioral performance as a result of repeated training of a visual stimulus, such as in a visual discrimination task (Watanabe and Sasaki, 2015). VPL

is retinotopically restricted because cortical representations in visual cortex are retinotopically mapped. Thus, VPL offers a reliable means to study changes in specific regions of neurons, allowing the observation of learning related changes in one area of cortex while providing within-subject controls of other areas of cortex outside of the retinotopic location of the visual stimulus. A handful of studies over the past few decades have investigated where along the visual processing hierarchy neural responses might adapt to support improved performance in these visually-guided tasks. However, findings surrounding changes in neural activity across learning in early visual cortex are conflicting, with some groups indicating changes occurring in primary visual cortex (V1) across several species - such as monkeys (Schoups et al., 2001; Yan et al., 2014), cats (Hua et al., 2010), rats (Hager and Dringenberg, 2010), and mice (Poort et al., 2015; Wang et al., 2016) - and others reporting no changes in monkey V1 or even in higher level areas such as V2 (Ghose et al., 2002; Yang and Maunsell, 2004).

Additionally, studies pertaining to changes in several higher order visual areas have provided mixed results. VPL-correlated changes have been described in visual area 4 (V4) (Yang and Maunsell, 2004; Raiguel et al., 2006) and a sensorimotor area (lateral intraparietal area, or LIP) thought to be responsible for transforming visual motion information into a motor choice via a saccade (Shadlen and Newsome, 2001; Law and Gold, 2008). On the other hand, no VPL changes were observed within a sensory area (medial temporal area, or MT) thought to represent motion information (Law and Gold, 2008). Last, two recent functional magnetic resonance imaging (fMRI) studies in humans have described VPL-associated effects occurring in subcortical and cortical regions. First, VPL-associated effects occurred within the lateral geniculate nucleus (LGN), a subcortical

region of the thalamus that receives a large number of afferent projections from the retina and projects strongly into V1 (Yu et al., 2016). Secondly, effects were described in visual area 3 (V3) and the connections between V3 and the intraparietal sulcus (IPS), a visual motion and motor-decision area (Chen et al., 2015).

### **Cortical and Subcortical Targets from Primary Visual Cortex**

Mixed results from VPL studies indicate neural changes may be occurring in a number of different areas in the brain. It remains unclear if changes are occurring in local areas of the cortex to support behavioral improvements or if changes occur solely downstream, such as in cortical association areas or subcortical regions. It is known that visual cortex has a high level of recurrent connectivity between excitatory neurons (Douglas et al., 1995). Changes originating in visual cortex to support learning could act as a means to amplify incoming signals for proper stimulus representation in downstream areas.

Alternatively, the stimulus representation in early cortex may remain constant throughout learning, with downstream areas adapting to more optimally filter such a stimulus for relevant behavior execution, perhaps involving a postsynaptic reweighting at the projections from V1 neurons to other regions (Dosher et al., 2013). Indeed, primary visual cortex contains a multitude of long-range efferent connections with many areas across the brain, potentially implicated in sensorimotor execution and perceptual learning. These areas have been mapped in both primates (Fellman and Van Essen, 1991) and, more recently, mice (Wang and Burkhalter, 2007). Intracortical areas specifically include projections to higher order visual areas such as posteromedial (PM) and anterolateral (AL)

cortex (Matsui and Ohki, 2013; Glickfield et al., 2013; Kim et al., 2018). Subcortical regions such as the LGN (Fitzpatrick et al., 1994; Briggs and Usrey, 2010) and the superior colliculus (SC) (Ito and Feldheim, 2018) also receive projections from V1. Additionally, it has been shown that individual neurons in V1 can project to multiple areas of the brain (Han et al., 2018).

### **Two-Photon Calcium Imaging and Optogenetic Tools**

Investigating the potential neural mechanisms underlying VPL in mammals requires a precise measure of the activity across many individual neurons *in vivo*. Traditional imaging methods, such as wide-field epifluorescence (one-photon) imaging, are unable to resolve the activity of single neurons, especially at depth, and modern *in vivo* electrophysiology methods are not scalable to many neurons or do not spatially disambiguate individual neurons (such as methods measuring local field potentials from the activity of multiple neurons surrounding the electrode). However, modern two-photon microscopy techniques allow for highly resolved imaging of many neurons at depth with a relatively greater signal-to-noise ratio than traditional imaging methods (Denk et al., 1990). This technique requires the emission and absorption of two photons of infrared light whose excitation energy superimposes to excite a wavelength specific fluorophore, as opposed to one-photon methods utilizing single photons of light at a specific wavelength. Additionally, two-photon methods are resistant to the scattering of photons through tissues, enabling high resolution depth sectioning.

Neuronal activity can be imaged via genetically-encoded calcium indicators, or GECIs (Mank and Griesbeck, 2008), which are fluorescently-labeled proteins that bind to

transient  $\text{Ca}^{+2}$  ions. These calcium indicators provide a measure of the transient calcium kinetics typical in active neurons through fluorescence (occurring on binding of  $\text{Ca}^{+2}$  ions) during a neuron's spiking. Due to their utility for chronically measuring activity of specific populations of neurons in living organisms, calcium indicators (e.g. GCaMP) have been heavily optimized (via targeted mutations and also forward genetic screening) to achieve greater sensitivity for reporting a neuron's spiking activity (Akerboom et al., 2013; Chen et al., 2013; for review see Badura et al., 2014).

Additionally, optogenetics provides a tool for precise control of the activity in a population of neurons. This level of control is critical for understanding learning related changes as it becomes possible to circumvent potential changes in stimulus representation in the cortex from an animal adjusting their gaze or position. For *in vivo* stimulation of neurons, opsins (such as channelrhodopsin or halorhodopsin) have proven to be a highly useful tool. Opsins are ion pumps or ion channels which absorb light and change a cell's electrical properties that can be expressed in targeted cells through genetic manipulations. These opsins allow for precise temporal control of excitable cells using a specific wavelength of light (Boyden et al., 2005).

Here, we target excitatory neurons in a local patch of cortex in mouse V1, which affords two key benefits: 1) animals can use non-natural, or “off-manifold” (Golub et al., 2018), activity patterns evoked via direct stimulation methods for behavior (Histed et al., 2013) and 2) mice provide a convenient model organism for facilitating the use of novel optogenetic tools to both image and stimulate neurons. We achieve cell-type specific expression of both a calcium indicator (e.g. GCaMP6f) and opsin (e.g. ChrimsonR) in excitatory neurons by taking advantage of the Cre/lox recombinase system (Gu et al.,

1993). Specifically, mouse lines can be bred with targeted genetic manipulations to express Cre in glutamatergic, excitatory neurons (Gorski et al., 2002; Harris et al., 2014). Targeted expression is thus accomplished using another genetic strategy: the flip-excision (FLEX) switch, which relies on site-specific recombinases of Cre and FLP to drive the expression of a FLEX viral construct in targeted cells expressing Cre (Atasoy et al., 2008). Through administration of injections of both a FLEX-ChrimsonR and FLEX-GCaMP6f viral construct in a glutamatergic-Cre mouse line, either Emx1-IRES-Cre (Gorski et al., 2002) or Slc17a7-IRES2-Cre (Harris et al., 2014), mice can be obtained which co-express the indicator and opsin in only glutamatergic neurons (Klapoetke et al., 2014; Chen et al., 2013). This combination thus allows for precise optical control of a neural population for consistent stimulus representation and a means to monitor the activity of the respective neural population chronically to assess potential changes in response properties of neurons as a result of learning, all within a local patch of cortex.

## HYPOTHESIS

As animals learn to detect optogenetically-evoked spiking in the visual cortex, bypassing upstream visual pathways, two hypotheses exist for how the brain might reorganize to support behavioral improvements. First, the optogenetically driven input applied to the cortex could be amplified by changes in local cortical circuitry over time. On the other hand, all the changes to support behavioral improvement could occur downstream of the cortex, perhaps in part due to synaptic reorganization at the synapses of neurons projecting out of the cortex. Using two-photon imaging techniques to monitor activity of neurons in V1 at the site of optogenetic stimulation, we can assess if learning-related changes take place in visual cortex to amplify stimulus signals (i.e. changes in tuning or response properties of local V1 neurons) or if all changes take place in downstream areas from visual cortex to improve behavioral performance (i.e. no changes measured in tuning or responses of local V1 neurons).

## **STUDY DESIGN**

Initially, transgenic mice were prepared for later behavior tasks and imaging via surgical implantation of a head-post for head-fixation and optical window for access to visualizing the cortex. Viral injections were administered during surgery to genetically co-express both the Cre-dependent FLEX-GCaMP6f calcium indicator and Cre-dependent FLEX-ChrimsonR opsin in V1 of transgenic mice expressing Cre in glutamatergic neurons. Following recovery from surgery and indicator and opsin expression maturation (2-3 weeks), mice were trained on a visual detection task. As behavior improved on this task, retinotopic imaging was performed to find the area in each animal's field of vision where a visual stimulus would maximally excite neurons at the location of opsin and indicator co-expression.

As animals continued to perform the visual detection task, a control stimulation experiment was performed. Two-photon calcium imaging of neuronal responses to directional visual stimuli was performed before and after 5 sessions of approximately 300 laser stimulations of the opsin at varying laser intensities (presented in random order), as outlined in Table 1.

Following the control experiment, animals began to train on an optogenetic stimulation detection task. Initially, the optogenetic stimulus (i.e. laser) was paired with the visual stimulus, where the visual stimulus was subsequently removed. Two-photon calcium imaging was performed again following training animals to detect the optogenetic

stimulus. All imaging was performed at both the site of optogenetic stimulation as well as a retinotopically-distinct control location which did not receive optogenetic stimulation throughout experiments. Behavioral and imaging experiments with animals are outlined in Figure 1. Analysis of behavior and neuronal responses followed completion of all experiments to quantify learning-related effects.

**Table 1: Laser intensities used across control stimulation experiments.** mW = milliWatts

Session	Laser Intensities (mW)
1	1.0, 0.48, 0.23, 0.11
2	1.0, 0.48, 0.23, 0.11
3	0.48, 0.23, 0.11, 0.054
4	0.48, 0.23, 0.11, 0.054
5	0.23, 0.11, 0.054, 0.026

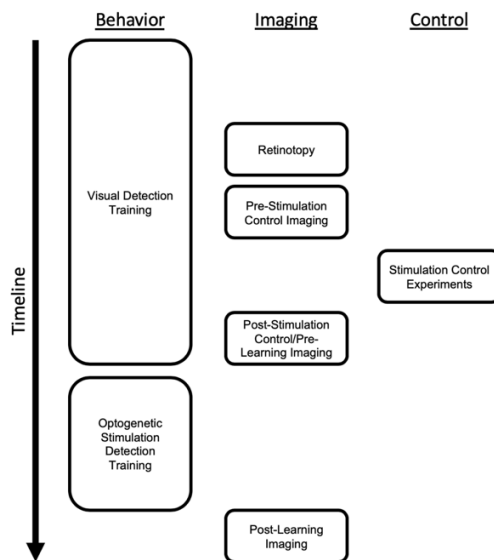


**Figure 1: Timeline of behavior, imaging, and control experiments.**

## **STUDY AIMS**

1. Train animals to reliably detect and report a novel, optogenetic stimulus in primary visual cortex and quantify learning related changes in behavior, i.e. improvements to stimulus sensitivity and improvements in reaction time.
2. Test whether learning-related changes occur in local cortical circuitry or if all changes to support behavioral improvements occur downstream by analyzing visual response properties of excitatory neurons at the site of stimulation before and after animals learn to detect an optogenetically-induced stimulus.

## METHODOLOGY

### Materials

Transgenic mouse lines (Jackson Laboratory; Bar Harbor, ME), Emx1 IRES-Cre (Stock No: 005628) and Slc17a7-IRES2-Cre (Stock No: 023527), virus vectors (Addgene; Watertown, MA), AAV9 Syn-FLEX-GCaMP6f-WRPE-SV40 (Catalog No: 100833) and AAV5 Syn-FLEX-ChrimsonR-tdTomato (Catalog No: 62723), air driven dental drill (Aseptico; Woodinville, WA), Neoburr drill bit (Friction Grip ¼ drill bit) (Microcopy; Kennesaw, GA), stereotactic syringe pump (Stoelting; Wood Dale, IL), custom metal head posts, optical windows (Tower Optical; Boynton Beach, FL), C&B Metabond dental cement (Parkell; Edgewood, NY), custom 3D-printed animal sleds, custom behavior rigs (parts from ThorLabs; Newton, NJ), monitor (VX238H, ASUS; Taipei, Taiwan), saccharin (Sigma-Aldrich; St. Louis, MO), Movable Objective Microscope (Sutter Instrument; Novato, CA), Mai Tai DeepSee Ti:Sapphire Laser (Spectra-Physics; Santa-Clara, CA), 16X Nikon CFI LWD plan fluorite objective (Nikon; Tokyo, Japan).

### Mouse Rearing and Surgical Preparation

Emx1-IRES-Cre and Slc17a7-IRES2-Cre (where IRES indicates internal ribosome entry site) mouse lines (Jackson Laboratory; Bar Harbor, ME) were used for targeted expression of Cre in excitatory, glutamatergic neurons to allow for localized co-expression of an injected double-floxed Cre-dependent calcium indicator (FLEX-GCaMP6f) and red-

shifted opsin (FLEX-ChrimsonR) in these neurons. Mice were anesthetized with isoflurane mixed in oxygen (2% during induction and 1.5% throughout surgery). Circular craniotomies of 3 mm diameter were performed to expose the left hemisphere of V1 (ML -3.1 mm relative to Lambda) using an air driven dental drill (Aseptico; Woodinville, WA) with a Neoburr drill bit (Friction Grip 1/4; Microcopy; Kennesaw, GA). Individual microinjections of viral vectors containing either a calcium indicator (AAV9-Syn-GCaMP6f-WPRE-SV40; Addgene; Watertown, MA) or a red-shifted opsin (AAV9-Syn-ChrimsonR-tdTomato; Addgene; Watertown, MA) were administered unilaterally using a stereotactic syringe pump (Stoelting; Wood Dale, IL) (Figure 2A). Injections of 500 nL were given at a rate of 0.1  $\mu$ L min<sup>-1</sup> 200  $\mu$ m beneath the surface of the brain. An optical window (3 mm diameter; Tower Optical; Boynton Beach, FL) was then implanted at the site of craniotomy. A custom metal head post was then implanted around the optical window. Both the optical window and head post were fixed to the skull using C&B Metabond dental cement (Parkell; Edgewood, NY). Following at least one week of recovery from surgery, mice were placed on a low-fat diet and restricted access to water for at least two weeks prior to and throughout behavioral tasks and imaging experiments.

### **Visual Detection Task**

The visual behavior task consisted of training mice to detect and report a visual grating stimulus within a specified window of time (Histed et al., 2012). Mice were placed in custom 3D-printed holding sleds and positioned into custom made behavior rigs (parts from ThorLabs; Newton, NJ) facing a monitor (240 mm away; 58.4 cm diagonal screen size) and head-fixed in order to prevent movement. A lever was placed directly in front of

animals to hold down and release on stimulus presentation and a tube for dispensing a saccharin (Sigma-Aldrich; St. Louis, MO) solution reward was positioned near their mouths (Figure 2C). Task trials were cued with an audio tone, at which point the animal was required to hold a lever down for a fixed amount of time (at least 600 ms) plus an additional random amount of time (0 - 3500 ms). Directly following this hold period, a visual stimulus was displayed across the entire monitor for a set amount of time. Early in training, the stimulus was displayed for 60 seconds, coinciding with the reaction time window for animals, but as training progressed this reaction time window was reduced to 550 ms with the stimulus only being flashed for 100 ms (Figure 2B). Additionally, the size of the stimulus is reduced from the full screen to a 25 x 25 cm Gabor patch at the center of the screen. If the animal released the lever prior to the visual stimulus appearing, the trial was deemed a false alarm, or early response. If the animal released the lever within the reaction time window, the trial was considered a hit, or a correct response. If the animal did not release the lever within the allotted reaction time window, the trial was considered a miss, or a failed response. Upon successful trials, the animal was supplemented with a small saccharin reward. If the trial resulted in a false alarm or miss, then the animal was required to wait an extra period of time before the next trial initiated. Between trials, there was an inter-trial interval of fixed time (0-5500 ms) with an additional amount of random time (0-1500 ms).

As animals mastered the task for a Gabor patch grating stimulus at full contrast (hit rate near 100% of trials), additional levels were added to lower the contrast and increase difficulty in detecting the visual stimulus in some trials. Animals were trained over several weeks until they performed at their detection threshold (i.e. contrast levels were reduced

until the animal was performing well at their highest contrast level, but poorly for their adjacent lower contrast levels without improvements over several training sessions). Last, the visual stimulus was slowly moved from the center of the screen to the retinotopic location corresponding to their designated one-photon stimulation training location in visual cortex.

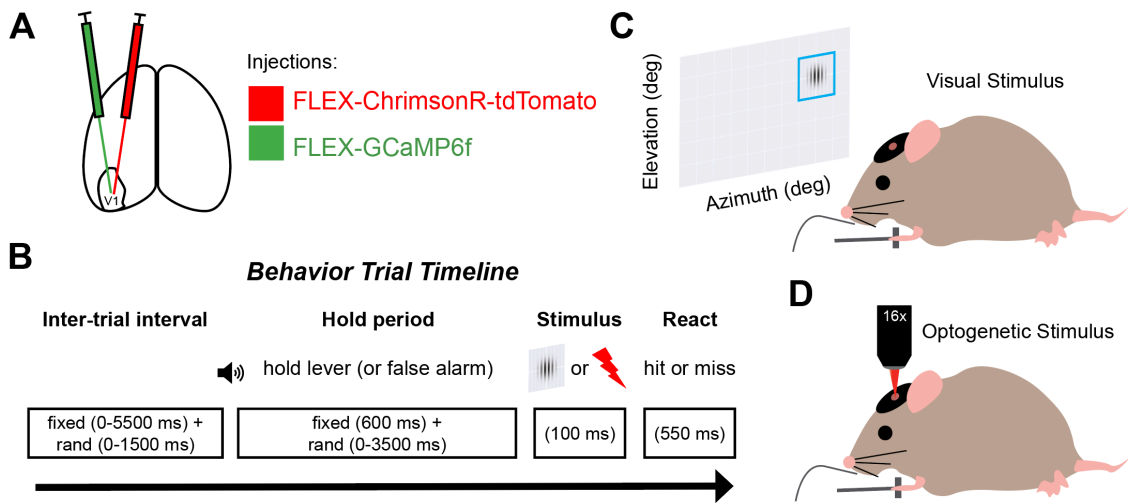


**Figure 2: Animal preparation and behavior task structure.** A) Injections of an opsin (FLEX-ChrismsonR) and a calcium indicator (FLEX-GCaMP6f) are administered unilaterally into V1 before beginning animals on a behavior task. B) The task structure consists of an inter-trial interval of a specified amount of time followed by a trial. An audio cue is presented to indicate the start of a trial, where an animal is required to hold a lever down, otherwise the trial will result in a false alarm. After a specified amount of time, the stimulus (either visual or optogenetic) is presented for 100 ms. The animal is required to respond by releasing the lever within a reaction time window for a correct response (hit). If the animal fails to respond, the trial results in a miss. C) The animal is initially trained to detect a visual stimulus presented on a monitor angled at 45 degrees and positioned contralaterally to the injected hemisphere. D) Eventually, animals are trained to detect an optogenetic stimulus (i.e. a laser pulse through an objective to excite the expressed opsin previously injected).

### Two-Photon Imaging

Two photon calcium imaging was conducted using a modified Moveable Objective Microscope (MOM; Sutter Instrument; Novato, CA) with a Mai Tai DeepSee Ti:Sapphire laser (Spectra-Physics; Santa-Clara, CA). Imaging was performed on head-fixed mice using a 16X water dipping objective (Nikon; Tokyo, Japan) attached to the MOM and manually positioned over the implanted optical window at the desired area in primary visual cortex. A small volume of saline solution was used to immerse the lens of the objective directly over the optical window. The imaging field of view (FOV) was 500 x 500 um and imaging was targeted to layers 2/3 of visual cortex (achieved by descending the focal plane of the objective between 150 - 200 um from the surface of the pia). Images of calcium responses were acquired at 5 Hz using ~50 mW laser power at 920 nm.

### **Retinotopy**

Retinotopic analysis via imaging (Scheutt et al., 2002) was performed in order to identify two locations in the animal's visual field that maximally excited the neurons at both the future one-photon stimulation training location (i.e. overlapping the opsin expression) and the control location (i.e. no opsin expression and approximately a millimeter away from training location in visual cortex to ensure the control area is retinotopically distinct from the training area). While imaging either the training or control location of visual cortex with two-photon calcium imaging, Gabor patch grating stimuli (15 x 15 cm, vertical orientation) were displayed repeatedly in multiple locations in a random order on a monitor sitting in front of the head-fixed animal at a 45-degree angle to the animal's right side (as in Figure 2C). Following imaging, the resulting image stack was divided according to the time frames where the position of the visual stimulus being

presented was the same and corresponding image frames were averaged to calculate the change in fluorescence over the baseline fluorescence in neurons resulting from the visual stimulus presentation ( $dF/F$ ). The retinotopic locations of the visual stimulus were selected for the training and control locations based on the stimulus position which excited the most neurons in the image FOV.

### **Visual Response Imaging**

Two-photon calcium imaging experiments were performed directly before and after training on the one-photon stimulation detection task to assess neural responses in visual cortex at both the training and control locations. Visual response imaging sessions were acquired at either cortical location by displaying stimuli on a monitor positioned in front of the head-fixed animals at a 45-degree angle to the animal's right side. The visual stimulus consisted of a 15 x 15 cm Gabor patch drifting grating stimulus at 100% contrast presented in 12 different directions (0 - 330 degrees, 30-degree increments) in random order for a total of 25 repetitions of each stimulus direction. During imaging sessions, a given direction-stimulus trial consisted of 4 seconds of no stimulus (20 pre-stimulus imaging frames) followed by a given direction stimulus displaying for 3 seconds (15 stimulus imaging frames). Gabor patch stimuli during imaging sessions were displayed on the monitor in the previously mapped retinotopic locations for training and control locations, respectively.

### **One-Photon Stimulation Detection Task**

Following visual detection task training and pre-learning imaging sessions, animals switched from a visual detection task to a one-photon stimulation detection task (Figure 2D). First, the visual stimulus (at the retinotopic location) was paired with a 100 ms laser pulse of 625 nm wavelength light illuminating a diameter of  $\sim$ 900 $\pm$ 200 microns across the cortex targeted at the training location. Laser power intensity was between 1 and 5 mW initially. With improved behavior, the visual stimulus was entirely removed with only the laser stimulus present. Similar to contrast levels in the visual detection task, decremented laser power levels were added as the animal improved performance over sessions. Animals used for pre- and post-learning imaging sessions trained on the task for approximately three weeks.

### **Behavioral Data Analysis**

Learning effects were characterized by analyzing data collected during animal behavior on the one-photon stimulation detection task. First, changes in reaction time across learning were analyzed for individual laser powers within the first few training sessions for each animal. For a given animal, behavior trials were grouped together by laser power. Only laser powers above 0.1 mW were used for reaction time analyses. Trials with laser powers within 10% of one another were grouped together. Reaction times were averaged across trials for each laser power group and for each training session. Linear fits were calculated for these data points across the start and end sessions in which each laser power group was present during the task. The slope of the linear fit indicated the change in reaction time per session for each laser power group. A mean change in reaction time per training session was then calculated across all laser powers for each animal. The median

change in reaction time across these population values was calculated and tested against the null hypothesis that no change in reaction time occurred during learning (median of zero) by using a one-sided Wilcoxon signed rank test. A p-value less than 0.05 denoted significance in reaction time changes.

Next, changes in detection sensitivity were analyzed by measuring the hit rate (the percentage of behavior trials resulting in a correct response) across trials grouped by laser power during a given training session. Weibull functions were fit to data from individual training sessions to estimate detection performance as a function of laser power. Inflection points in the fitted functions were used to define laser power detection thresholds for a given training sessions.

Mean changes in false alarm rates (i.e. the percentage of behavior trials resulting in an early response) were calculated for each animal using the same methods described above for reaction time.

### **Image Analysis and Spike Inference**

Visual response imaging data was initially analyzed using the open-source software CaImAn (Giovannucci et al., 2019). CaImAn uses a constrained nonnegative matrix factorization (CNMF) method to estimate segmentation of neural components in the FOV across the entire image set, separate the neural components from the background component (eg. widespread neuropil activation in the FOV), and extract the raw calcium signal fluorescence traces for each of the identified neural components. Additionally, CaImAn uses these neural component traces in time to calculate an inferred proxy for the spiking events,  $a \cdot S(t)$ , of the neural components using the decay constant of the

fluorescent signal from the calcium indicator in the sample. The decay constant of GCaMP6f is approximately 400 ms (Chen et al., 2013). Using the approximation that trial-to-trial variability in neuronal spiking in the cortex is roughly predicted by a Poisson process (Tolhurst et al., 1981; Carandini, 2004), we can estimate the mean spike count is nearly equivalent to the variance of the spike count:

$$\text{mean}(S) \approx \text{VAR}(S).$$

With this assumption, we can estimate the unknown coefficient of the inferred spiking returned via CaImAn to normalize the spike count:

$$\text{mean}(a \cdot S) = a \cdot \text{mean}(S),$$

$$\text{VAR}(a \cdot S) = a^2 \cdot \text{VAR}(S),$$

$$\text{mean}(a \cdot S)/a \approx \text{VAR}(a \cdot S)/a^2,$$

$$a \approx \frac{\text{VAR}(a \cdot S)}{\text{mean}(a \cdot S)},$$

$$S_{norm} = a \cdot S(t)/a.$$

Last, we multiply  $S_{norm}$  by the imaging rate of 5 Hz to yield spikes per second, or the inferred spike rate of each neural component.

Custom software was constructed using the Python programming language to further analyze neural responses to visual stimuli.

### **Visual Response Analysis - Direction Stimuli**

For each neural component in the FOV, raw fluorescence traces and inferred spike rates were divided up according to like-stimulus trials (individual directions) and averaged across trial frames to calculate trial-average responses. Tuning curves denoting the

response to each direction stimulus were calculated by first averaging the average spike rates across a fraction of the imaging frames directly preceding the stimulus presentation (baseline activity, 15 frames) and across all directions, and then subtracting this baseline value from the average spike rates across all of the imaging frames where the stimulus was present for each direction (response, 15 frames). Tuning curves were then used to calculate a metric for responsivity (the sum of all response points along the tuning curve, or summed response) as well as orientation and direction selectivity to quantify the tuning properties of individual neural components. Previously published methods were adopted for calculating a direction selectivity index (DSI) and a global orientation selectivity index (gOSI) and between 0 and 1, where 0 indicates no selectivity and 1 indicates maximal selectivity for a given stimulus direction or orientation (preferential neural response to a particular direction and its opposite direction) (Kondo and Ohki, 2016).

To quantify the preferred direction of a neural component, a circular double Gaussian function (von Mises function) was fit to the respective tuning curve. The peak of the fit was considered the preferred direction. Linear interpolation was performed between data points on the tuning curve surrounding the peak of the fit in order to define the response value in the preferred direction. The DSI was then calculated using the following equation:

$$DSI = \frac{R_{pref} - R_{opp}}{R_{pref} + R_{opp}},$$

where  $R_{pref}$  was the response in the preferred direction,  $\theta_{pref}$ , and  $R_{opp}$  was the response in the opposite direction,  $\theta_{opp} + \pi$ . To calculate the gOSI of a neural component, a vector averaging method was utilized (Swindale, 1998):

$$a = \sum R_i \sin 2\theta_i,$$

$$b = \sum R_i \cos 2\theta_i,$$

$$\text{and } gOSI = \sqrt{a^2 + b^2} / \sum R_i,$$

where  $R_i$  is the response for a given stimulus direction,  $\theta_i$ .

DSI, gOSI, and summed response values across the population of neural components for various stages of imaging (refer to Figure 1) at a respective imaging location (training or control locations) were compared using the Kolmogorov-Smirnov two sample test. A p-value less than 0.05 was used to indicate significant differences in the population metrics between imaging sessions.

## RESULTS

### **Reaction Times Decrease as Animals Learn to Detect an Optogenetic Stimulus**

In order to understand the effects of learning on cortical responses in early visual cortex, animals (N=9) expressing opsin in excitatory neurons were trained to detect and report an optogenetic stimulus applied directly to V1. Initially, to begin training animals to detect this optogenetic stimulation, the stimulus was paired with the prior visual stimulus. Shortly after, the visual stimulus was removed entirely, and animals reported only the optogenetic stimulus. As animals performed consistently at high laser intensities, more levels of lower laser intensity were added. All levels present within the first few training sessions where a marked reduction in the mean reaction time occurred (respective to individual animals; see Table 2) were analyzed individually to assess changes in reaction time as a function of the number of training sessions (Figure 3A). Specifically, linear fits were applied to mean reaction times for individual laser intensities pooled across the first several training sessions without the visual stimulus, where the slopes of the fits represent the mean change in reaction time per training session, normalized to the range of training sessions for each animal. Results indicate that animals tend to decrease their reaction time by a median $\pm$ SEM of approximately  $-15.9\pm3.8$  ms per training session across their initial learning period ( $p<0.01$ ; Wilcoxon signed rank test against a median of zero; Figure 3B). Altogether, by observing the mean change in reaction time per session for each

animal's number of sessions analyzed (Table 2), we find a mean $\pm$ SEM total reduction in reaction time during training of  $-89.3\pm20.1$  ms.

**Table 2: Reaction time analysis parameters for individual animals**

Animal	Laser Intensities in Analysis	Number of Training Sessions in Analysis	Mean Change in Reaction Time per Session	No. Sessions x Mean Change in Reaction Time per Session
A	6.5, 2.43, 1.75, 1.26, 0.91, 0.65, 0.47, 0.34, 0.24, 0.18, 0.13	8	-18.2	-145.6
B	5.0, 3.6, 2.59, 1.87, 1.27, 0.83, 0.5, 0.4	4	-6.9	-27.6
C	0.58, 0.42, 0.3, 0.22, 0.16, 0.11	5	-31.2	-156.0
D	1.0, 0.48, 0.35, 0.22, 0.1	5	2.7	13.5
E	1.0, 0.72, 0.52, 0.37	5	-12.6	-63.0
F	0.36, 0.26, 0.19, 0.13	9	-15.9	-143.1
G	0.8, 0.6, 0.48, 0.32, 0.23, 0.17	5	-27.6	-138.0
H	0.75, 0.54, 0.39, 0.28, 0.2, 0.14, 0.1	7	-8.0	-56.0
I	1.0, 0.48, 0.23, 0.11	3	-29.4	-88.2

The reduction in reaction time characterized here could arise from two possibilities. First, the animal could be gradually improving on the task, establishing more proficiency in detecting or decoding the stimulus signal induced in the cortex. Second, the animals could be adjusting their timing strategy on the behavior task. Because of the task structure,

animals could begin to respond faster after the audio cue denoting the start of each trial. Such a timing strategy may improve their chances of getting correct responses earlier after

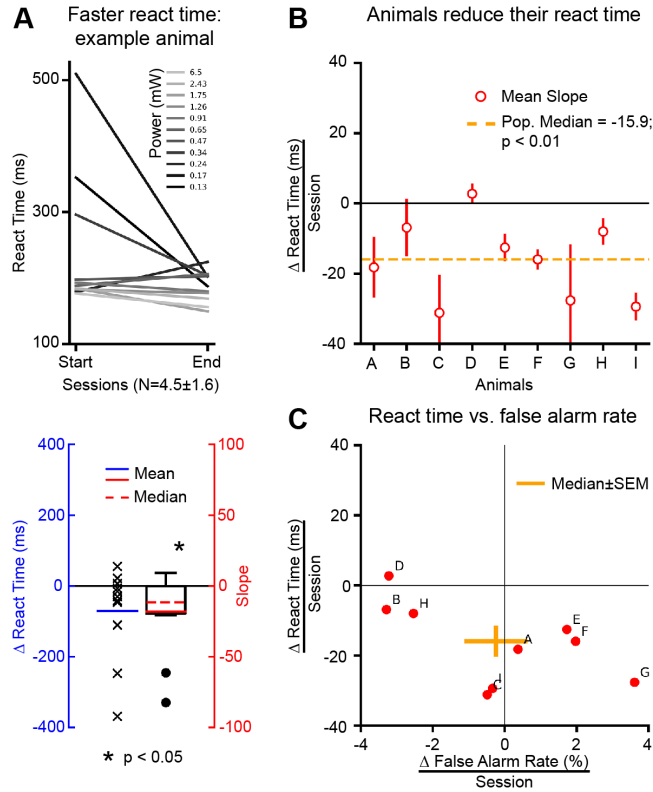


**Figure 3: Animals reduce their reaction time to optogenetic stimuli early in learning.** A) Top panel: Linear fits of reaction time data across sessions for individual laser powers ( $N=4.5\pm 1.6$ , mean $\pm$ SEM number of sessions each laser power was present) are shown for an example animal. Reaction times drop across sessions for a majority of laser powers. Bottom panel: The change in reaction time (end - start) is depicted for each laser power (blue) for the same example animal. Values normalized to the number of sessions a power was present are equivalent to the slopes of each linear fit (red). The boxplot depicts the upper and lower quartile values of the slopes with outliers plotted as points. The median slope value indicates a significant reduction in reaction time across powers ( $p<0.05$ , tested against null hypothesis of a zero median using Wilcoxon signed rank test). B) Mean $\pm$ SEM reaction time slopes (i.e. change in reaction time per session) were plotted for individual animals ( $N=9$ ). The population median $\pm$ SEM (-15.9 $\pm$ 3.8 ms) was tested against a median of zero in order to quantify significance in reaction time reductions across all animals that learned the task ( $p<0.01$ , Wilcoxon signed rank test). C) Mean change in false alarm rates per session were quantified similarly to reaction time to test if an increase in early responses from animals would explain reaction time reductions. The change in false alarm rate per session across the population of animals did not significantly vary ( $p>0.05$ , Wilcoxon signed rank test).

the stimulus is displayed but will also result in more false alarms (or releasing the lever before the stimulus appears). In order to assess if reductions in reaction time were caused by improved learning or by a change in the animal's timing strategy, we analyzed false alarm rates across the same sessions used in the prior analysis for individual powers for each animal, respectively. Using the same approach to find the mean change in reaction time per session, we calculated the mean change in false alarm rates per session for each animal and calculated the median $\pm$ SEM across the population of animals (Figure 3C). Our findings indicate that animals did not significantly change their timing strategy and support the claim that animals do gradually improve their performance at detecting the optogenetic stimulus.

### **Animals Improve Sensitivity to Optogenetic Stimulation as Training Progresses**

While we have characterized the short-term learning effect of a reduction in reaction time as animals transition to the optogenetic detection task, we also observed animals were able to improve their sensitivity to the laser stimulus over many training sessions. Since multiple levels of laser powers were used within a given training session in some animals, we were able to analyze behavioral performance as a function of the stimulus intensity. For two example animals, we generated fits (see Methods) across the hit rates at each laser power within a given training session to establish a psychometric function of the animal's performance (Figure 4A). Sensitivity thresholds to the laser intensity were defined as the inflection point in the psychometric curve. By comparing these fits at various points along an example animal's training sessions, we found there was

a continued decrease in detection threshold many sessions out ( $>90$  sessions) with sensitivity improving by over an order of magnitude. Changes in detection threshold could also be confounded by shifts in the animal's behavior strategy, however, example animals' performance remained roughly constant over training sessions throughout this time, as stimulus intensity was reduced (Figure 4B). These results suggest animals are able to continue improving their ability to detect the optogenetic stimulus many days out.

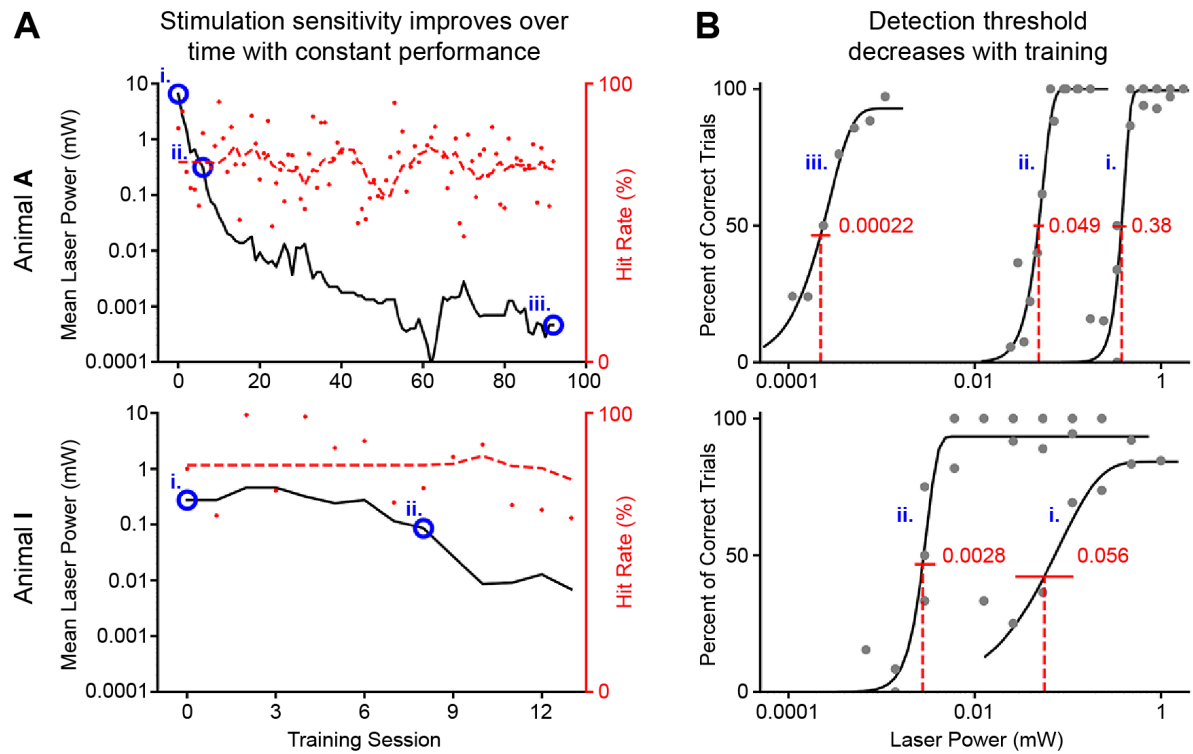


**Figure 4: Sensitivity to stimulus intensity improves across learning.** A) Example animals depict a steady hit rate (percent of trials performed correctly) across multiple training sessions as laser powers are reduced. B) Psychometric thresholds to laser power decrease across training, indicating an improvement in sensitivity to the laser stimulus.

## **Neuron Responses in V1 Adapt to Support Learning of an Optogenetic Stimulus**

Observing that animals can learn to detect an optogenetic stimulation and are able to improve their ability in detection on both short- (reaction time reduction) and long-term (sensitivity improvement) scales, we hypothesized changes in the brain must occur to support either a more optimal stimulus representation in the cortex (i.e. changes occurring in V1) or a more optimal means of decoding the stimulus (i.e. changes occurring downstream). In order to investigate potential learning-related effects in the brain, we analyzed responses in excitatory neurons within V1 at the site of optogenetic stimulation before and after learning. Utilizing two-photon calcium imaging techniques, we imaged responses of these neurons to drifting grating stimuli retinotopically aligned to the area of visual cortex targeted for laser stimulation or a control location (Figure 5A). Using software to extract calcium traces and inferred spike rates from individual neuronal components in the FOV, we calculated trial-averaged responses to the drifting grating stimulus moving in each of twelve directions (Figure 5B). Tuning curves for each neuron were then calculated from the trial-averaged responses by taking the difference between the average spike rates during stimulus and baseline periods in order to assess direction and orientation tuning, as well as responsivity (Figure 5C). These tuning curves were used, in turn, to calculate three various metrics to measure across the population of neurons in the FOV: a direction selectivity index (DSI), a global orientation selectivity index (gOSI), and the sum of the response differences across all directions (i.e. a measure of the overall responsiveness of a neuron to any direction visual stimulus). Comparing distributions of these metrics across neurons in the same patch of cortex for both the training and control locations before and after an animal (N=1) learned to detect the optogenetic stimulus

revealed that population shifts occur at the training location, but not at the control location (Figure 6). Furthermore, these shifts denote overall decreases in direction ( $p<0.05$ ; Kolmogorov-Smirnov two sample test) and orientation ( $p<0.05$ ; Kolmogorov-Smirnov two sample test) selectivity, but an increase in the responsiveness of neurons to any visual stimulus ( $p<0.01$ ; Kolmogorov-Smirnov two sample test).

Because changes in neural responses were only observed at the training location, we asked if these changes were induced by learning to detect the optogenetic stimulus, or if these changes were a result of repeated stimulation of the opsins in the imaged neurons. To answer this question, we repeatedly stimulated an area of V1 neurons expressing opsin for five sessions with varying laser intensity (see Table 1) in another animal and conducted the same imaging experiments in the stimulation location. Here, we find that repeated stimulation of opsin does not produce any significant shifts in DSI, gOSI, or responsiveness ( $p>0.05$ ; Kolmogorov-Smirnov two sample test) at the stimulation location (Figure 7).

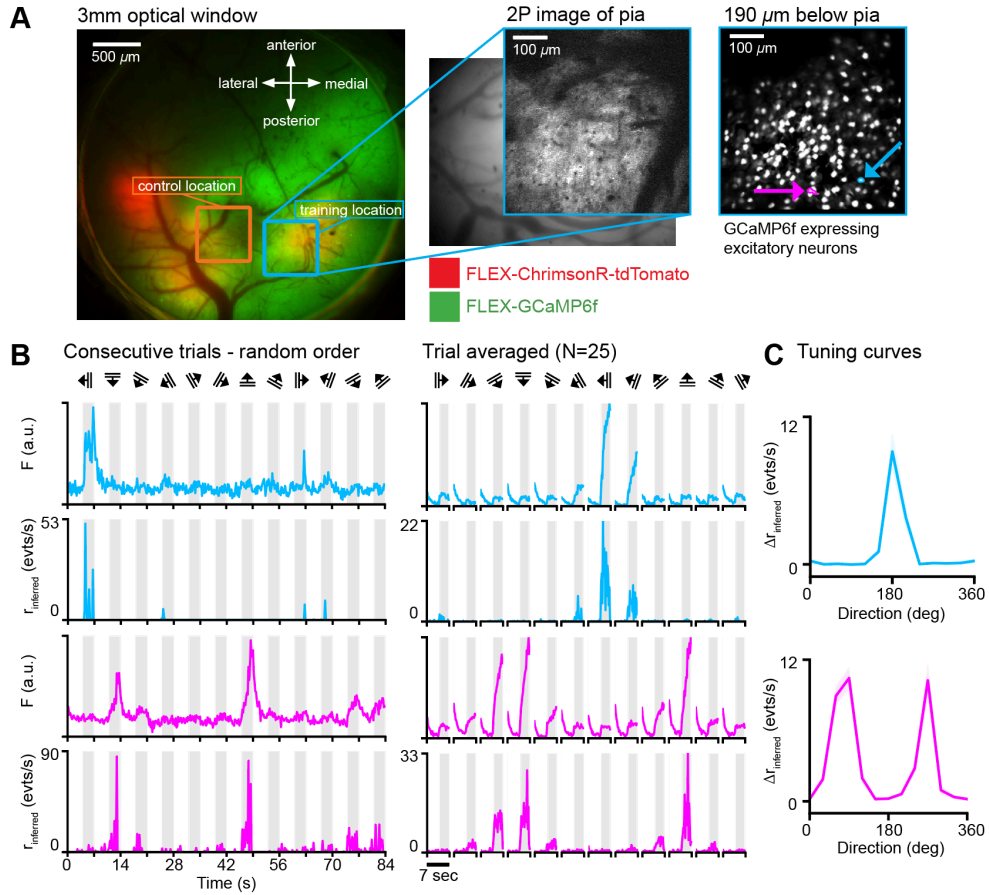


**Figure 5: Two-photon calcium imaging of neuron responses to visual stimuli allow quantification of tuning properties.** A) Imaging was performed at both the training (blue) and a control (orange) location to analyze neuron responses to various directional visual stimuli. Imaging was performed by locating a region using widefield epifluorescence, matching the location of the surface during live two-photon imaging and descending the objective approximately 180-200 microns to position the focal plane in layer 2/3 of cortex. B) Individual neurons (two example neurons indicated in blue and magenta) were analyzed to assess responses to each of twelve direction stimuli via raw fluorescence and inferred spike rates. (Left) Twelve direction stimuli are displayed in random order across consecutive trials for two neurons in the FOV. Groups of consecutive trials covering all stimulus directions were repeated 25 times. (Right) Trial-averaged responses were calculated across all repetitions for a given stimulus direction. C) Tuning curves were calculated as the difference between the mean spike rate during imaging frames when the stimulus was present and the mean spike rate during the imaging frames before the stimulus was present (baseline activity) for each direction.

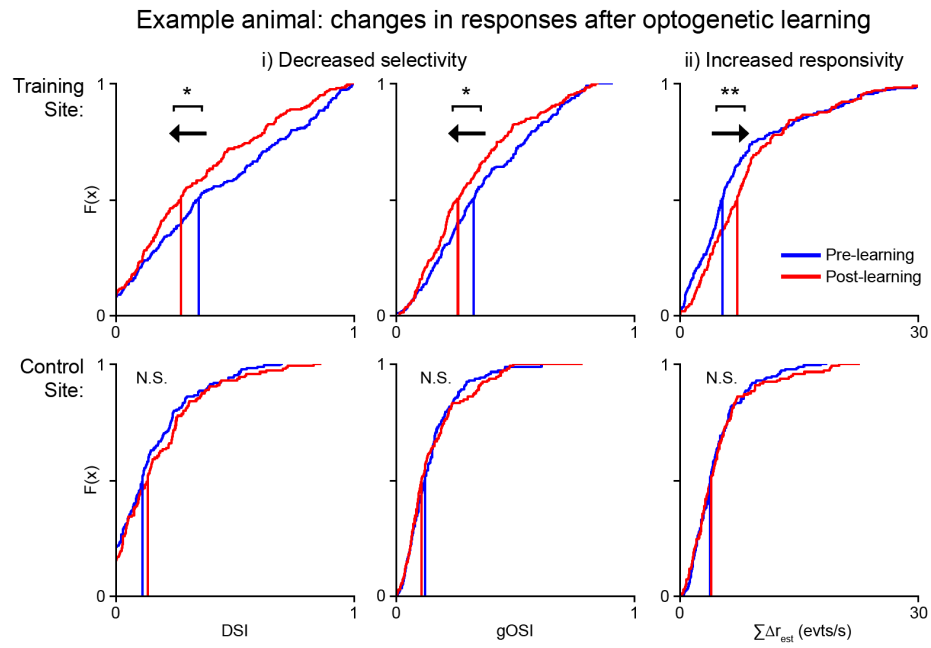


**Figure 6: Learning an optogenetic stimulus induces changes in V1 neuron selectivity and responsivity at the site of stimulation.** Cumulative distribution functions (CDFs) of DSI, gOSI, and summed response values for all neurons imaged before and after learning in both the training (N=226 pre-learning, N=218 post-learning) and the control (N=174 pre-learning, N=144 post-learning) sites. Shifts in CDFs at the training location indicate population level decreases in selectivity (DSI or gOSI; \* p<0.05; Kolmogorov-Smirnov two sample test) and increases in responsivity (summed response; \*\* p<0.01; Kolmogorov-Smirnov two sample test). No significant shifts (p>0.05; Kolmogorov-Smirnov two sample test) were found in selectivity or responsivity at the control site before and after learning.

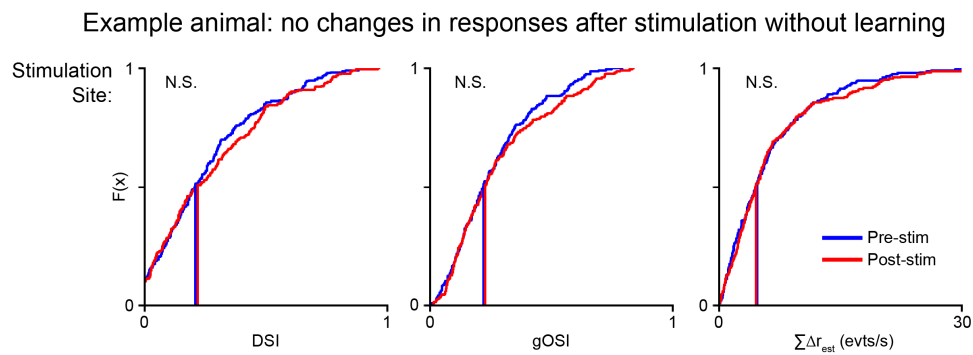


**Figure 7: Repeated stimulation of opsin does not induce changes in selectivity or responsivity in V1 neurons.** CDFs of DSI, gOSI, and summed response across neurons imaged before (N=236) and after (N=229) repeated optogenetic stimulation do not indicate population-level shifts in selectivity or responsivity (p>0.05; Kolmogorov-Smirnov two sample test).

## DISCUSSION

In this study, we show mice can learn to detect an optogenetically-induced stimulus in excitatory neurons of primary visual cortex and that behavioral improvements occur over time. A prior study has demonstrated that mice can indeed learn to detect optogenetic stimulation alone in the olfactory bulb via patterned two-photon holographic illumination techniques (Lerman et al., 2018). Such techniques lend scientists a novel tool to achieve unprecedented control of neuronal activity *in vivo* and allow for opportunities to understand and dissect the mechanisms underlying the pathways from sensory processing to eventual behavioral output. Here, we demonstrate how this optogenetic control can be used to investigate visual sensory processing in a learning paradigm, wherein animals are trained for many sessions to detect local cortical stimulation, and thus completely bypassing upstream visual processing areas.

First, we characterized behavioral learning effects in trained mice. Results show that mice adjust their reaction time during the first few sessions of receiving solely the optogenetic stimulation by approximately  $-89.3 \pm 20.1$  ms. Typical visual stimuli must propagate from the retinal ganglion cells and through the thalamus (i.e. LGN) before projecting to V1. The reductions in reaction time shown here are thought to be a cause of the stimulus being applied directly to V1, and suggests animals are reliant on the initial spiking activity in early cortex for behavior. While our stimulus does bypass upstream visual processing areas, this does not conclusively indicate interactions with these areas are not responsible for changes seen in the response profiles of the layer 2/3 neurons to visual

stimuli. Indeed, primary visual cortex consists of reciprocal projections with the thalamus (Briggs and Usrey, 2010), which could act to modulate local corticocortical interactions, thereby changing neuronal responses in V1 as measured using visual stimuli. Thus, it will be important to characterize potential changes in local cortical responses to optogenetic stimuli, whether through one-photon excitation or two-photon patterned illumination, to understand the magnitude of changes occurring at the local cortical level versus modulation from top-down feedback. Such changes to optogenetic stimulation in individual neurons may reveal mechanisms at the neuron or circuit level to support an improved sensitivity to lower stimulus intensities. Indeed, we observed mice were able to improve their detection sensitivity to lower laser powers across many sessions, perhaps providing a means to track gradual changes in neuron responses throughout learning.

Detection of an optogenetic stimulus in this behavioral paradigm may be the direct result of the amplification of a pre-reinforced network change induced by visual learning before the optogenetic detection task, as opposed to *de novo* learning of the optogenetic stimulus. However, this is unlikely the case as the optogenetic stimulation evokes a synchronous, non-specific increase in excitation across many V1 neurons. While this excitation may amplify the signal from a pre-reinforced network, it is likely that many other neurons add noise to the evoked signal, forcing animals to learn an entirely new pattern of activity in the cortex. The shifts characterized in selectivity and responsivity occurring only after learning the optogenetic stimulus support this hypothesis as it remains unclear from prior literature if learning a visual stimulus drives robust changes in local cortical responses. Training animals solely on the optogenetic stimulus without prior visual training may indicate if amplifying a pre-reinforced network is critical for detection of the

optogenetic stimulus. However, this remains a difficult endeavor as the visual detection task lends us considerable flexibility in the visual stimulus to familiarize an animal with the task structure, while the one-photon stimulation is far more rigid and perceptually difficult, introducing numerous challenges for learning early in the task.

Prior studies have provided a range of results in regard to potential changes in visually-evoked neuronal responses before and after learning. Studying visual perceptual learning effects has implicated multiple areas in adapting to support learning, including V1 and several downstream targets. In mice, changes have been reported in V1 to learning visual stimuli, although complex task structures convolute the interpretation of some of the reported changes. For example, Wang et al. (2016) demonstrate the dendritic spine density of neurons in V1 increase after learning. However, the task involved was a two-alternative, forced-choice visual discrimination task requiring animals to associate a grating stimulus with escaping from water. Such a task introduces a number of confounding factors, such as motor action through swimming or increased levels of stress from potential drowning. These factors cannot be dismissed when interpreting changes in cortex, as such changes could be driven from outside the context of learning in the animals. Learning of a similarly complex task structure has been linked to changes in V1 of mice in another study (Poort et al., 2015), although results indicate only modest effects on slopes of tuning curves after learning. Again, subtle shifts in tuning properties of V1 neurons were demonstrated early in macaques through an orientation discrimination task (Schoups et al., 2001). Further studies using a slightly adjusted behavioral task indicated no changes in V1 response properties (Ghose et al., 2002). To further convolute these results, electrode recordings used do not allow for precise measurements of tuning in individual neurons.

To control for these issues, we use here a simple, structured detection task (Histed et al., 2012) allowing for psychophysical measurements of stimulus sensitivity, a consistent optogenetic stimulus applied to the same region of cortex, and two-photon imaging methods to measure the response properties of many individual neurons. By training mice to detect an optogenetic stimulus applied directly to V1, we provide early evidence that neuronal responses in visual cortex adapt to support improved detection of a stimulus, characterized by decreases in direction and orientation selectivity across the population and increases in responsivity to any direction visual stimulus, perhaps as a mechanism to improve sensitivity to the stimulus in behavior. Altogether, these changes do not appear to be widespread across V1 and are not caused solely from repeated opsin excitation, but rather are driven by learning at the local site of stimulation.

## CONCLUSION

Animals can improve their behavior after repetition of sensory stimuli. Such sensory processing requires thousands of neurons from many different areas of brain. Here, we asked whether or not improvements in behavior to a specific stimulus were the result of changes in local cortical responses (changes in local neurons' tuning or responsivity to stimuli) or if all changes to support this improvement occurred downstream (no changes in local neuronal tuning or responsivity). Using optogenetic strategies to target stimulation directly to excitatory cells in early visual cortex, we found animals were able to enhance their performance; characterized by a reduction their reaction time for reporting the stimulus and a gradual increase in their sensitivity to the stimulus intensity. Additionally, using a calcium indicator expressed in excitatory neurons, we investigated potential population shifts in neuronal selectivity and responsivity to visual stimuli before and after learning an optogenetic stimulus. Our results posit shifts do occur in these properties at the site of stimulation, but only in the context of learning. Specifically, neurons stimulated at the training location decrease selectivity to specific visual stimuli (e.g. direction and orientation), but overall, increase their responsivity to any stimuli. Conversely, neurons at a retinotopically distinct location not stimulated during behavior do not change their selectivity or responsivity after learning occurs. Repeated stimulation outside the context of learning also does not change the selectivity or responsivity of neurons. Altogether, this study suggests changes do occur in local cortical responses to support learning a new

stimulus. In order to understand if structural network changes are occurring in local cortical circuitry or in downstream areas to drive local adaptations in cortical responses to visual stimuli, it will be imperative to understand how the activity in local V1 neurons change in response to the training stimulus (widefield optogenetic excitation). Future studies will aim to replicate these findings in more animals and to investigate potential changes in downstream areas to further our understanding of sensory processing in the brain.

## REFERENCES

1. Akerboom J et al. (2013) Genetically encoded calcium indicators for multi-color neural activity imaging and combination with optogenetics. *Front Mol Neurosci* 6:2.
2. Atasoy D, Aponte Y, Su HH, Sternson SM (2008) A FLEX switch targets Channelrhodopsin-2 to multiple cell types for imaging and long-range circuit mapping. *J Neurosci* 28:7025–7030.
3. Badura A, Sun XR, Giovannucci A, Lynch LA, Wang SS-H (2014) Fast calcium sensor proteins for monitoring neural activity. *Neurophotonics* 1:025008.
4. Boyden ES, Zhang F, Bamberg E, Nagel G, Deisseroth K (2005) Millisecond-timescale, genetically targeted optical control of neural activity. *Nat Neurosci* 8:1263–1268.
5. Briggs F, Usrey WM (2007) A fast, reciprocal pathway between the lateral geniculate nucleus and visual cortex in the macaque monkey. *J Neurosci* 27:5431–5436.
6. Carandini M (2004) Amplification of Trial-to-Trial Response Variability by Neurons in Visual Cortex Charles Stevens, ed. PLoS Biol 2:e264.
7. Chen N, Bi T, Zhou T, Li S, Liu Z, Fang F (2015) Sharpened cortical tuning and enhanced cortico-cortical communication contribute to the long-term neural mechanisms of visual motion perceptual learning. *Neuroimage* 115:17–29.
8. Chen T-W, Wardill TJ, Sun Y, Pulver SR, Renninger SL, Baohan A, Schreiter ER, Kerr RA, Orger MB, Jayaraman V, Looger LL, Svoboda K, Kim DS (2013) Ultrasensitive fluorescent proteins for imaging neuronal activity. *Nature* 499:295–300.
9. Denk W, Strickler JH, Webb WW (1990) Two-photon laser scanning fluorescence microscopy. *Science* 248:73–76.
10. Dosher BA, Jeter P, Liu J, Lu Z-L (2013) An integrated reweighting theory of perceptual learning. *Proc Natl Acad Sci U S A* 110:13678–13683.
11. Douglas RJ, Koch C, Mahowald M, Martin KA, Suarez HH (1995) Recurrent excitation in neocortical circuits. *Science* 269:981–985.
12. Felleman DJ, Van Essen DC (n.d.) Distributed hierarchical processing in the primate cerebral cortex. *Cereb Cortex* 1:1–47.

13. Fitzpatrick D, Usrey WM, Schofield BR, Einstein G (1994) The sublaminar organization of corticogeniculate neurons in layer 6 of macaque striate cortex. *Vis Neurosci* 11:307–315.
14. Ghose GM, Yang T, Maunsell JHR (2002) Physiological Correlates of Perceptual Learning in Monkey V1 and V2. *J Neurophysiol* 87:1867–1888.
15. Giovannucci A, Friedrich J, Gunn P, Kalfon J, Brown BL, Koay SA, Taxidis J, Najafi F, Gauthier JL, Zhou P, Khakh BS, Tank DW, Chklovskii DB, Pnevmatikakis EA (2019) CaImAn an open source tool for scalable calcium imaging data analysis. *Elife* 8.
16. Glickfeld LL, Andermann ML, Bonin V, Reid RC (2013) Cortico-cortical projections in mouse visual cortex are functionally target specific. *Nat Neurosci* 16:219–226.
17. Gold JI, Watanabe T (2010) Perceptual learning. *Curr Biol* 20:R46–8.
18. Goldstone RL (1998) Perceptual learning. *Annu Rev Psychol* 49:585–612.
19. Golub MD, Sadtler PT, Oby ER, Quick KM, Ryu SI, Tyler-Kabara EC, Batista AP, Chase SM, Yu BM (2018) Learning by neural reassociation. *Nat Neurosci* 21:607–616.
20. Gorski JA, Talley T, Qiu M, Puelles L, Rubenstein JLR, Jones KR (2002) Cortical excitatory neurons and glia, but not GABAergic neurons, are produced in the Emx1-expressing lineage. *J Neurosci* 22:6309–6314.
21. Gu H, Zou YR, Rajewsky K (1993) Independent control of immunoglobulin switch recombination at individual switch regions evidenced through Cre-loxP-mediated gene targeting. *Cell* 73:1155–1164.
22. Hager AM, Dringenberg HC (2010) Training-induced plasticity in the visual cortex of adult rats following visual discrimination learning. *Learn Mem* 17:394–401.
23. Han Y, Kebschull JM, Campbell RAA, Cowan D, Imhof F, Zador AM, Mrsic-Flogel TD (2018) The logic of single-cell projections from visual cortex. *Nature* 556:51–56.
24. Harris JA, Hirokawa KE, Sorensen SA, Gu H, Mills M, Ng LL, Bohn P, Mortrud M, Ouellette B, Kidney J, Smith KA, Dang C, Sunkin S, Bernard A, Oh SW, Madisen L, Zeng H (2014) Anatomical characterization of Cre driver mice for neural circuit mapping and manipulation. *Front Neural Circuits* 8:76.
25. Histed MH, Carvalho LA, Maunsell JHR (2012) Psychophysical measurement of contrast sensitivity in the behaving mouse. *J Neurophysiol* 107:758–765.
26. Histed MH, Ni AM, Maunsell JHR (2013) Insights into cortical mechanisms of behavior from microstimulation experiments. *Prog Neurobiol* 103:115–130.

27. Hua T, Bao P, Huang C-B, Wang Z, Xu J, Zhou Y, Lu Z-L (2010) Perceptual learning improves contrast sensitivity of V1 neurons in cats. *Curr Biol* 20:887–894.
28. Ito S, Feldheim DA (2018) The Mouse Superior Colliculus: An Emerging Model for Studying Circuit Formation and Function. *Front Neural Circuits* 12:10.
29. Karni A, Sagi D (1991) Where practice makes perfect in texture discrimination: evidence for primary visual cortex plasticity. *Proc Natl Acad Sci U S A* 88:4966–4970.
30. Kim M-H, Znamenskiy P, Iacaruso MF, Mrsic-Flogel TD (2018) Segregated Subnetworks of Intracortical Projection Neurons in Primary Visual Cortex. *Neuron* 100:1313–1321.e6.
31. Klapoetke NC et al. (2014) Independent optical excitation of distinct neural populations. *Nat Methods* 11:338–346.
32. Kondo S, Ohki K (2016) Laminar differences in the orientation selectivity of geniculate afferents in mouse primary visual cortex. *Nat Neurosci* 19:316–319.
33. Law C-T, Gold JI (2008) Neural correlates of perceptual learning in a sensory-motor, but not a sensory, cortical area. *Nat Neurosci* 11:505–513.
34. Lerman GM, Gill J V, Rinberg D, Shoham S (2018) Precise optical probing of perceptual detection. *bioRxiv*:456764.
35. Mank M, Griesbeck O (2008) Genetically Encoded Calcium Indicators. *Chem Rev* 108:1550–1564.
36. Matsui T, Ohki K (2013) Target dependence of orientation and direction selectivity of corticocortical projection neurons in the mouse V1. *Front Neural Circuits* 7:143.
37. Ni AM, Maunsell JHR (2010) Microstimulation reveals limits in detecting different signals from a local cortical region. *Curr Biol* 20:824–828.
38. Poort J, Khan AG, Pachitariu M, Nemri A, Orsolic I, Krupic J, Bauza M, Sahani M, Keller GB, Mrsic-Flogel TD, Hofer SB (2015) Learning Enhances Sensory and Multiple Non-sensory Representations in Primary Visual Cortex. *Neuron* 86:1478–1490.
39. Raiguel S, Vogels R, Mysore SG, Orban GA (2006) Learning to see the difference specifically alters the most informative V4 neurons. *J Neurosci* 26:6589–6602.
40. Schoups A, Vogels R, Qian N, Orban G (2001) Practising orientation identification improves orientation coding in V1 neurons. *Nature* 412:549–553.
41. Schuett S, Bonhoeffer T, Hübener M (2002) Mapping retinotopic structure in mouse visual cortex with optical imaging. *J Neurosci* 22:6549–6559.

42. Shadlen MN, Newsome WT (2001) Neural Basis of a Perceptual Decision in the Parietal Cortex (Area LIP) of the Rhesus Monkey. *J Neurophysiol* 86:1916–1936.
43. Swindale NV (1998) Orientation tuning curves: empirical description and estimation of parameters. *Biol Cybern* 78:45–56.
44. Tolhurst DJ, Movshon JA, Thompson ID (1981) The dependence of response amplitude and variance of cat visual cortical neurones on stimulus contrast. *Exp Brain Res* 41–41:414–419.
45. Wang Q, Burkhalter A (2007) Area map of mouse visual cortex. *J Comp Neurol* 502:339–357.
46. Wang Y, Wu W, Zhang X, Hu X, Li Y, Lou S, Ma X, An X, Liu H, Peng J, Ma D, Zhou Y, Yang Y (2016) A Mouse Model of Visual Perceptual Learning Reveals Alterations in Neuronal Coding and Dendritic Spine Density in the Visual Cortex. *Front Behav Neurosci* 10:42.
47. Watanabe T, Sasaki Y (2015) Perceptual Learning: Toward a Comprehensive Theory. *Annu Rev Psychol* 66:197–221.
48. Yan Y, Rasch MJ, Chen M, Xiang X, Huang M, Wu S, Li W (2014) Perceptual training continuously refines neuronal population codes in primary visual cortex. *Nat Neurosci* 17:1380–1387.
49. Yang T, Maunsell JHR (2004) The Effect of Perceptual Learning on Neuronal Responses in Monkey Visual Area V4. *J Neurosci* 24:1617–1626.
50. Yu Q, Zhang P, Qiu J, Fang F (2016) Perceptual Learning of Contrast Detection in the Human Lateral Geniculate Nucleus. *Curr Biol* 26:3176–3182.

## **BIOGRAPHY**

Paul Kristian LaFosse graduated from Eastern Randolph High School in Ramseur, North Carolina in 2011. He received his Bachelor of Arts in Physics from the University of North Carolina at Chapel Hill in 2015 and is pursuing a Master's Degree in Biology at George Mason University. He intends to pursue a Doctorate in Neuroscience in the future.